We are IntechOpen, the world's leading publisher of Open Access books Built by scientists, for scientists

4,800
Open access books available

122,000
International authors and editors

135M
Downloads

Our authors are among the

154
Countries delivered to

TOP 1%
most cited scientists

12.2%
Contributors from top 500 universities

CLARIVATE ANALYTICS BOOK CITATION INDEX INDEXED

WEB OF SCIENCE™

Selection of our books indexed in the Book Citation Index in Web of Science™ Core Collection (BKCI)

Interested in publishing with us?
Contact book.department@intechopen.com

Numbers displayed above are based on latest data collected.
For more information visit www.intechopen.com

7

Efficacious Considerations for the Design of Diffusion Controlled Pesticide Release Formulations

Steven A. Cryer,
Dow AgroSciences LLC,
USA

1. Introduction

Registration of a pesticide in today's regulatory climate requires environmental friendliness in addition to efficacy against the target pest. Most modern pesticides have rapid environmental degradation rates to meet this former constraint. Efficacy is often correlated with the product of environmental concentration (C) and contact time (T) as an indirect measure of the exposure an organism experiences ($C \times T$). If the pesticide degrades rapidly within the environment, then the time window (contact time) for pest control/efficacy can be small, and controlled release devices are often used with rapidly degradable or volatile pesticides to create an effective half-life within the environment that is longer than the degradation half-life of the pesticide alone.

Various physical methods to construct pesticide micro-encapsulations exist such as pan and air-suspension coating, centrifugal extrusion, vibration nozzle and spray drying. Chemical methods include interfacial, in-situ, and matrix polymerization, with interfacial polymerization a widely used method with pesticides. Interfacial polycondensation deals with the reaction of a monomer at the interface between two immiscible liquid phases to form an encapsulating film of polymer surrounding the disperse phase. Readily available polycondensates are polyureas, polyurethanes, polyamides, polysulphonamides, polyesters and polycarbonates, and descriptions of pesticide release from various microcapsules are found elsewhere (Allan et al, 1971; Dailey et al, 1993; Akelah, 1996; Dowler et al, 1999; Quaglia et al, 2001; Dailey, 2004; Asrar et al, 2004).

Determining the amount of pesticide from microcapsule sources within an environmental matrix is a two step process that includes diffusion from the controlled release device followed by degradation and dissipation of previously released material within the environment. The release rate is a function of the pesticide ingredient, polymer membrane properties, size of the device, and environmental concentration gradients. Release rates can be affected by physical constraints such as sunlight, water, soil pH, and capsule clustering, and knowledge of the mass of a pesticide in an environmental matrix such as soil, air, or water is mandatory for determining release rates, biological efficacy, and the potential for non-point source pollution. Physically based mathematical models are provided to address pesticide release loss from micro-capsule formulations, subsequent environmental degradation, and the impact on release characteristics when capsule clustering occurs.

2. Diffusion model development

Figure 1 represents an idealized spherical capsule where pesticide is encapsulated by a polymer membrane. Pesticide must first diffuse across the membrane before becoming available for biological impact or subject to environmental dissipation mechanisms. The pesticide concentration within the capsule is greatest immediately following application and decreases with time as mass diffuses across the membrane. Characteristic length scales for diffusion include the membrane thickness and the environmental length scale associated with the pesticide transport distance once released. Numerous historical and mathematical descriptions for pesticide loss from microcapsules can be found elsewhere (Carslow and Jaeger, 1959; Collins and Doglia, 1973; Collins, 1974; Kydenieus, 1980, Coswar, 1981; Crank, 1993; Mogul et al, 1996)

C = concentration of pesticide within the capsule (assumed uniform throughout capsule).
C_o = initial concentration of pesticide within the capsule for $t \leq 0$.
C_s = concentration of pesticide at the membrane-environmental interface.
C_∞ = concentration of pesticide within the environment that is not impacted by the contribution from the capsule (typically equal to zero).
L = characteristic length scale for resistance to mass transfer within the environmental matrix where $C_{ext} \sim C_\infty$.
C_{ext}= concentration of pesticide outside the membrane wall and within the environment
a = capsule radius.
h = membrane thickness.
t = time.

What follows is a rudimentary, classical first-principles (conservation equations) approach for determining release rates from capsule release devices (Collins, 1974). The concentration of the pesticide at the membrane/environment interface (C_s) is approximately zero if mass transport away from the capsule is sufficiently rapid, leaving diffusion of pesticide across the membrane under these conditions as the rate-limiting step for environmental release.

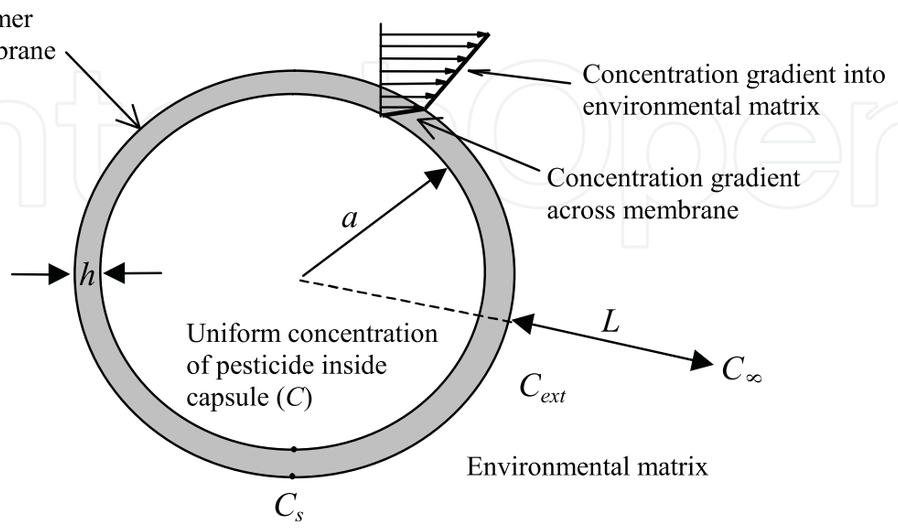

Fig. 1. Idealized cross-section of a spherical microcapsule.

The appropriate boundary condition at the membrane-environment interface is given by equating the mass flux loss from the membrane to the flux gain into the environment (Eq. 1);

$$D_m[\frac{\partial C}{\partial r}_{r=a+h}]_m = -D_{env}[\frac{\partial C}{\partial r}_{r=a+h}]_{env} \quad (1)$$

where:

D_m = diffusion coefficient of pesticide through membrane [cm^2 s^{-1}]

D_{env} = diffusion coefficient of pesticide through environmental matrix (air, soil, water) [cm^2 s^{-1}]

$[\frac{\partial C}{\partial r}_{r=a+h}]_m$ = concentration gradient of pesticide through membrane evaluated at the membrane-environment interface ($r=a+h$)

$[\frac{\partial C}{\partial r}_{r=a+h}]_{env}$ = concentration gradient of pesticide through environmental matrix evaluated at the membrane-environment interface ($r=a+h$).

The pesticide concentration gradients in the boundary condition of Eq. 1 are approximated as linear which, upon simplification, yields the concentration of pesticide at the membrane-environmental matrix interface (C_s).

$$C_s = \frac{C_\infty + \{\frac{D_m}{D_{env}}\frac{L}{h}\}C}{1+\{\frac{D_m}{D_{env}}\frac{L}{h}\}} = \frac{C_\infty + \alpha C}{1+\alpha} \quad (2)$$

where

$\alpha = \frac{D_m}{D_{env}}\frac{L}{h}$.

The parameter α is a measure of the relative diffusion magnitudes across the membrane and the environment. If the resistance to mass transfer within the environment is small (D_{env} >> D_m) then $\alpha = 0$ and Eq. 2 reduces to $C_s = C_\infty$.

The rate of diffusion (F) from the capsule across the membrane is given by Fick's first law

$$F = -D_m \frac{\partial C}{\partial r} = D_m \frac{(C - C_s)}{h} \quad (3)$$

where

F = Rate (flux) at which pesticide passes through the membrane [g cm^{-2} s^{-1}]

$\frac{\partial C}{\partial r}$ = Concentration gradient in radial direction across the membrane.

If one assumes the capsule keeps its spherical shape as pesticide is released through the membrane, the diffusion flux can also be represented as the rate of mass transport (g s^{-1}) across the surface area of the spherical capsule (A). The mass of pesticide inside the membrane is the volume (V) multiplied by the concentration (C). Thus,

$$F = -\frac{d}{dt}(\frac{VC}{A}) = \frac{d}{dt}(\frac{\frac{4}{3}\pi a^3 C}{4\pi a^2}) = -\frac{a}{3}\frac{dC}{dt} \quad (4)$$

where the volume and surface area of a sphere have been substituted. Equating Eq. 3 and Eq. 4 (and assuming C_∞ = 0), yields, upon simplification, a first order, separable, homogeneous ordinary differential equation, which simplifies to

$$\frac{dC}{dt} = -\frac{3\,D_m C}{a\,h(1+\alpha)}\,. \tag{5}$$

The solution to Equation 5 is

$$\frac{C(t)}{C_0} = \frac{M(t)}{M_0} = e^{-(\frac{3\,D_m}{a\,h})\frac{1}{(1+\alpha)}t} = e^{-0.693\frac{t}{\tau}} \tag{6}$$

where

$$\tau = 0.693\ \frac{a\,h(1+\alpha)}{3D_m}\,. \tag{7}$$

Equation 6 can be multiplied by the capsule volume to yield the mass remaining within the capsule. Therefore the dimensionless concentration ($\frac{C(t)}{C_0}$) or mass ($\frac{M(t)}{M_0}$) can be used interchangeably (since the capsule is assumed to remain spherical and of constant size over time). $M(t)$ is the mass of pesticide remaining within the capsule, and M_0 is the initial pesticide mass inside the capsule before diffusion losses begin. Here, τ is the half-life for release and is a function of the diffusion coefficient (D_m), membrane thickness (h), and capsule radius (a). τ will increase as the capsule radius, membrane thickness, and/or the parameter α increases and as the diffusion coefficient across the membrane decreases (Eq. 7). The diffusion loss from the capsule decreases as the mass transfer resistance in the environmental matrix increases ($\alpha\uparrow$, Figure 2). The actual amount of pesticide released from the capsule [$M_r(t)$] is determined by difference since the initial starting mass (M_0) is known and the mass at any time "t" [$M(t)$] is given by Eq. 6.

$$M_r(t) = M_0 - M_0\ e^{-0.693\frac{t}{\tau}} = M_0\,(1 - e^{-0.693\frac{t}{\tau}}). \tag{8}$$

Pesticide is often exposed to degradation and/or dissipation processes once outside of the capsule. Mechanisms for release and degradation/dissipation can be represented using a box model (Figure 3). Here, Q and R are the mass of pesticide inside and outside the capsule, respectively, and S represents the breakdown products of the pesticide. The mass of pesticide in the environment (i.e., R) is required from an efficacy standpoint. Thus, the material balance for R is written as

$$\frac{dR}{dt} = r_Q - r_R \tag{9}$$

where
r_Q = rate of mass transport of pesticide inside capsule to capsule surface/environment
r_R = rate of degradation of pesticide once outside capsule and in the environment.

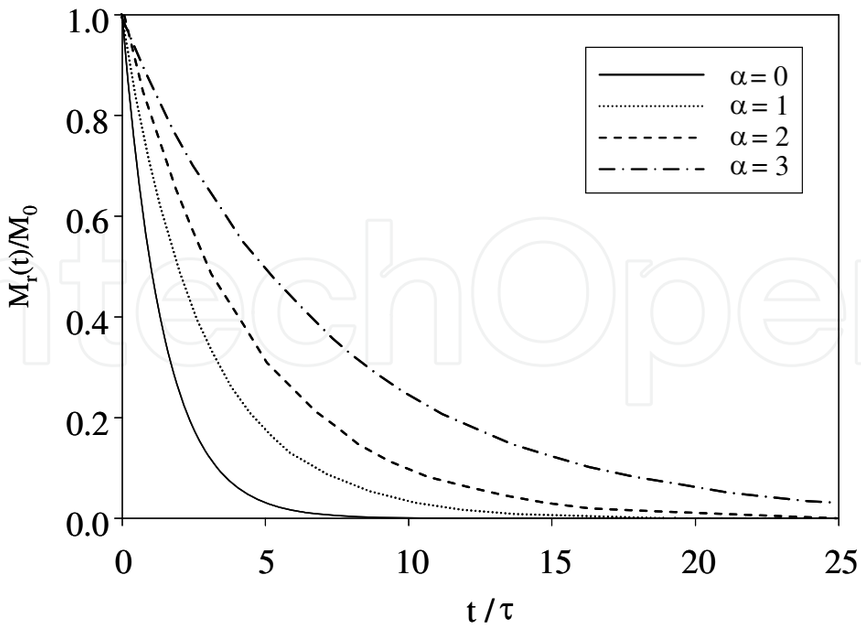

Fig. 2. Dimensionless mass of pesticide remaining in an idealized capsule as a function of time (dimensionless).

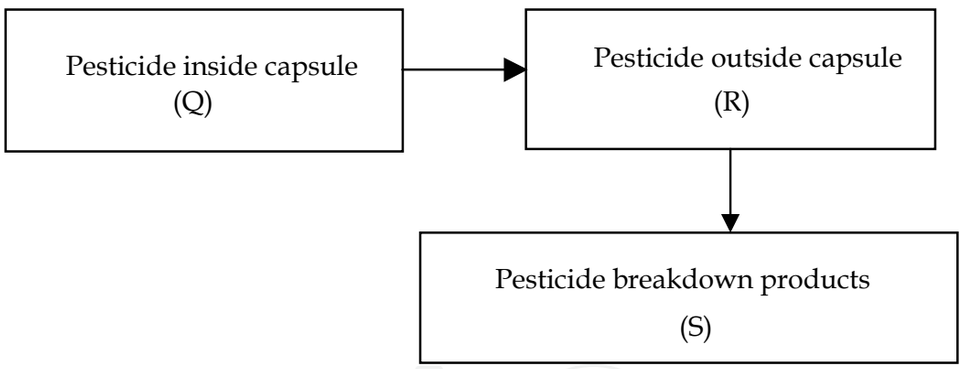

Fig. 3. Simple box model describing release rate and degradation of pesticide in the environment.

The rate of change of mass within the capsule (mass release rate, $\dot{M}_t$) is obtained by differentiating Equation 6 with respect to time.

$$\dot{M}_t = \frac{0.693 M_0}{\tau} e^{-0.693\frac{t}{\tau}} = r_Q \tag{10}$$

which is the rate of change represented by r_Q in the mass balance equation (Eq. 9). If the rate of degradation for pesticide once released into the environment is assumed to follow first order kinetics, then Eq. 9 can be written as

$$\frac{dR}{dt} + kR = \frac{0.693 M_0}{\tau} e^{-0.693\frac{t}{\tau}}. \tag{11}$$

Eq. 11 is a first order ordinary differential equation that can be integrated through an appropriate choice of an integration factor. Here, $\tau_o = \frac{0.693}{k}$ is the degradation half-life of the pesticide within the environment. The solution to Eq. 11 is

$$\frac{R}{M_0} = \frac{1}{(\frac{\tau}{\tau_o} - 1)} e^{-0.693\frac{\tau}{\tau_o}(\frac{t}{\tau})} \{e^{0.693(\frac{\tau}{\tau_o}-1)\frac{t}{\tau}} - 1\} . \quad (12)$$

For $\frac{\tau}{\tau_0} < 1$, diffusion dominates environmental degradation. Similarly, for $\frac{\tau}{\tau_0} > 1$, degradation dominates diffusion. The maximum mass in the environment is achieved after an initial lag time has elapsed (Figure 4). This lag time can be alleviated by adding a conventional formulation (e.g., emulsion where the pesticide mass from a conventional formulation is assumed immediately available for biological impact following the application). The conventional pesticide formulation has no controlled release characteristics (eq., $\tau = 0$). The mass of pesticide in the environment is the sum of pesticide from the conventional formulation (with degradation processes occurring) and the amount released from the microcapsule formulation at any given time, Equation 13.

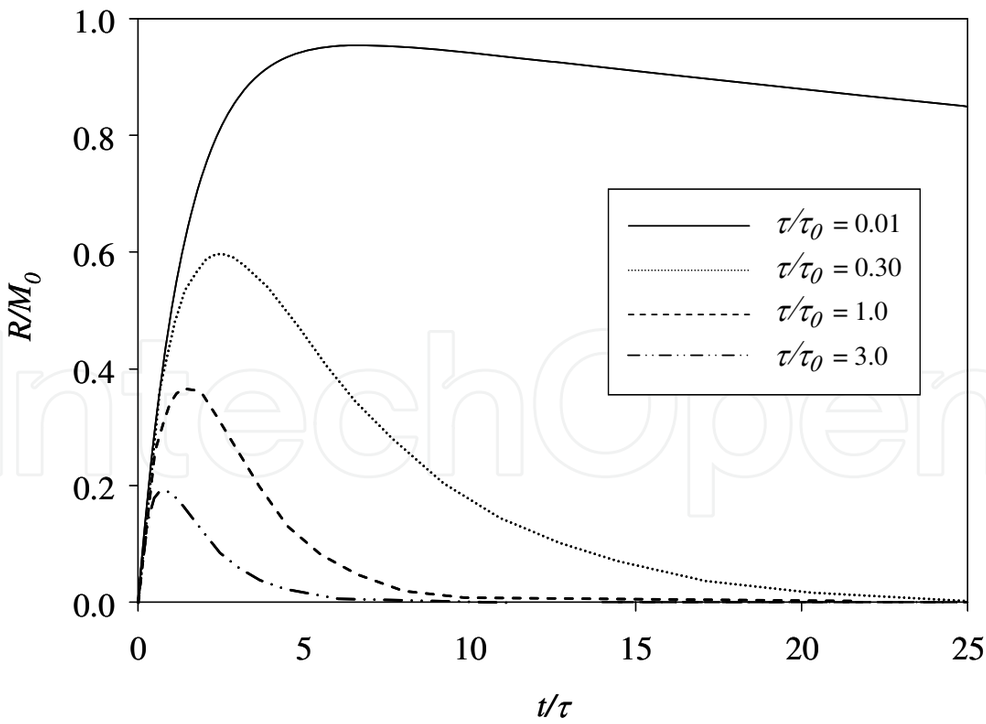

Fig. 4. Example of pesticide mass in the environment (R/M_0) for various ratios of capsule to degradation half-lives (τ/τ_0) as a function of time (t/τ).

$$R = [M_{conv} - \frac{M_0}{(\frac{\tau}{\tau_o} - 1)}]e^{-0.693\frac{\tau}{\tau_o}(\frac{t}{\tau})} + \frac{M_0}{(\frac{\tau}{\tau_o} - 1)}e^{-0.693(\frac{t}{\tau})} \quad (13)$$

where M_{conv} equals the initial mass of conventional formulation added to the system.
Properties for the solute/polymer interactions can be related by various constitutive relationships such that polymer specific attributes of the membrane can also be specified (Muro-Sune et al, 2005a, 2005b).
Equation 13 illustrates the capability of a hybrid microcapsule system (microcapsules, conventional formulation) to control the effective half-life of the pesticide within the environment, governed by capsule release characteristics (τ) as opposed to environmental degradation properties (τ_o). This provides a clear example of the ability of altering the effective degradation (and thus persistence) of a pesticide via controlled release devices, where the effective degradation half-life in the environment can be a function of manufacturing parameters such as the capsule radius and membrane thickness.
Equation 13 can be made non-dimensional by representing the amount of conventional formulation (M_{conv}) as a fraction of the controlled release formulation (M_0), with $\beta = \frac{M_{conv}}{M_0}$.

Since the total mass applied is

$$M_{t0} = M_{conv} + M_0 = M_0(1+\beta), \quad (14)$$

then Eq. 13 reduces to

$$\frac{R}{M_{t0}} = \frac{1}{(1+\beta)}[\beta - \frac{1}{(\frac{\tau}{\tau_o} - 1)}]e^{-0.693\frac{\tau}{\tau_o}(\frac{t}{\tau})} + \frac{1}{(\frac{\tau}{\tau_o} - 1)}e^{-0.693(\frac{t}{\tau})} \quad (15)$$

Examples of predicted environmental concentrations (dimensionless, Eq. 15) for pesticide released from a hybrid capsule formulation [for different formulation input parameters defining the capsule (τ), environmental degradation (τ_0), and the ratio of conventional to controlled release formulations (β)] as a function of dimensionless time (t/τ) is provided in Figure 5.

3. Polydisperse capsule size distribution

The previous analysis quantifies release patterns for a single capsule of constant radius and membrane thickness with results characterized in terms of a system release half-life (τ). However, during manufacturing processes, capsule sizes and membrane thickness can and do vary and thus release characteristics for the "effective" controlled release formulation can be different. As a first approximation, a heterogeneous capsule mixture can be approximated as a series of independent monodisperse mixture of capsules, where each capsule size releases mass as governed by Equation 12.
The mass fraction (f_i) for capsules of radius a_i is defined as:

$$f_i = \frac{\frac{4}{3}\pi a_i^3 g_i \rho_{capsule}}{\frac{4}{3}\pi \rho_{capsule} \sum_{i=1}^{N_b} a_i^3} = \frac{a_i g_i}{\sum_{i=1}^{N_b} a_i^3} \quad (16)$$

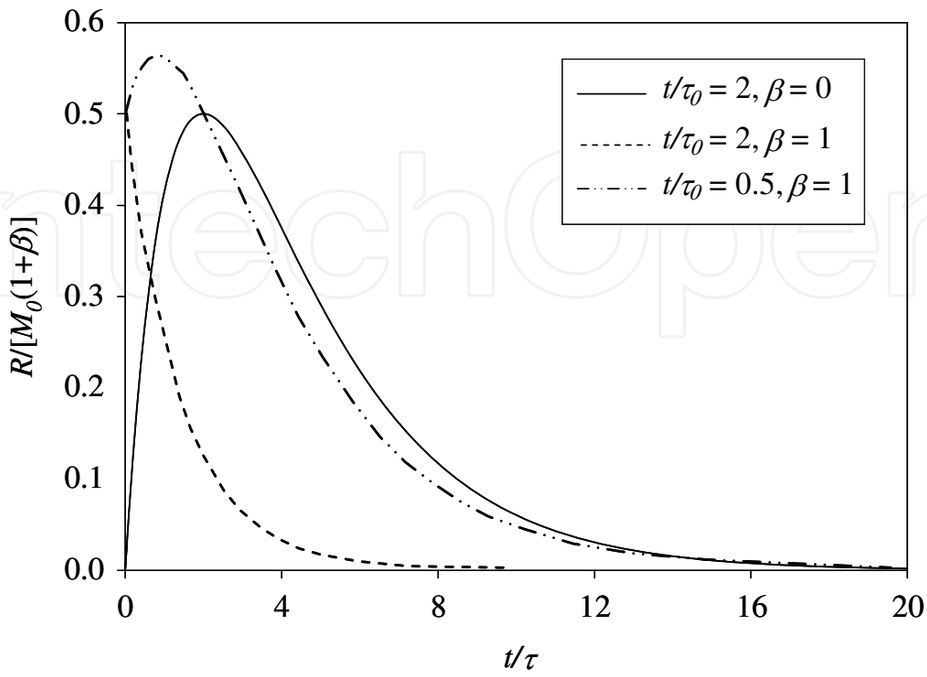

Fig. 5. Example of mass of pesticide in the environment for various ratios of capsule to degradation half-lives and conventional formulation addition ($\beta > 0$).

where

g_i = frequency (volume weighting) for capsules of size a_i (and membrane thickness h_i) within the distribution

f_i = mass fraction of capsule "i" size = (mass of capsules of size a_i)/ (total mass of all sizes).

The total amount of pesticide mass remaining within the capsule, assuming each capsule size (a_i, h_i) emits pesticide characterized by Equation 12, is the sum remaining for each unique, discrete capsule size distributions. The dimensionless scaling term γ has been added to account for different application rates for the pesticide. For γ = 1, then the scaled application rate is used. For γ = 2, then twice the scaled application rate is used, and so on. Here, M_{t0} is now defined as the total pesticide mass from all capsule sizes within the system at the time of application.

$$\frac{R}{\gamma M_{t0}} = \frac{1}{(1+\beta)}\{\sum_{i=1}^{n} f_i([\beta - \frac{1}{(\frac{\tau_i}{\tau_o}-1)}]e^{-0.693\frac{\tau_i}{\tau_o}(\frac{t}{\tau_i})} + \frac{1}{(\frac{\tau_i}{\tau_o}-1)}e^{-0.693(\frac{t}{\tau_i})}])\} \quad (17)$$

4. Application of single capsule diffusion equation

Characterizing pesticide release rates from microcapsules and relating them to biological observations provides an avenue to use mathematical models to design optimal release rate

characteristics that yield maximum impact on the target pest (e.g., efficacy). To illustrate this principle, biological information and microcapsule release characteristics for a commercial herbicide for both a target (weed) and non-target plant (crop) species are determined via appropriate experimental observations, Figure 6. Linear regression lines have been drawn through each data set. Clearly, as the capsule release half-life increases, both target and non-target species injury decreases, and ideally, injury to non-target species should be minimal. However, efficacy will suffer as reductions in injury to non-target species are sought. The slope found in Figure 6 for the target species (e.g., weed) is greater than the slope for the non-target species. Thus, a change in τ has a more significant impact on weed species than the non-target species, and a conceptual optimal microcapsule release profile is anticipated that can maximize efficacy against the weed while minimizing injury to the non-target species.

A release half-life of approximately 400 hours is appropriate for this experimental data set if the goal is to have at least 90% control of the weed species (e.g., Figure 6). However, experiments used to generate Figure 6 were performed in controlled environments within a greenhouse where the dominant mode of dissipation for this herbicide (aqueous photolysis) did not occur. A laboratory aerobic aquatic degradation study yielded a half-life of 21 days, and an average soil dissipation half-life of 3.5 days for this herbicide. Thus, degradation is more rapid under field conditions then in the greenhouse where efficacy information was collected.

The modeling algorithm previously outlined can be useful to aid in formulation development. For this example, τ = 400 hours, but the anticipated degradation half-life once released is τ_0 = 504 hours (21 days) under aerobic, aquatic conditions. Assume five different capsule size distributions are available, as characterized by different size radius, to construct the optimal release profile, Figure 7. All distributions are log-normal, characterized by different means and standard deviations for capsule diameters. Capsule distribution mean radius values range from 2-200 μm, respectively. The diffusion coefficient across the membrane used was 3.6×10^{-13} cm^2 hr^{-1} and the membrane thickness (h_i) was approximated as 0.001 times the capsule radius (a_i). Thus, larger microcapsules had a thicker polymer membrane than smaller microcapsules.

The goal is to maximize efficacy while minimizing injury to the non-target crop, which simplifies to a mixing scenario where the unknowns are the volumes or mass fractions for each microcapsule size component (e.g., distributions 1-5, Figure 7). Mass fraction combinations of the different formulations were determined by a Levenburg-Marquardt procedure to minimize the sum of the squared residuals (ψ) between the greenhouse-measured optimal release profile (e.g. τ = 400 hours) and the predicted release patterns (Eq. 15 with β = 0) at selected time intervals 'i".

$$\psi = \sum_{i=1}^{n} (\text{Biological Observation}_i - \text{Predicted}_i)^2 \tag{18}$$

n = number of discrete time intervals over the mass release interval.

The greenhouse-determined optimal pesticide release pattern that maximized efficacy but minimized non-target plant injury is provided in Figure 8 (i.e., τ = 400 hrs, τ_0 = 21 days), along with two different "optimal" combinations of capsule mass fractions for the test problem. Here, the actual environmental degradation half-life is set equal to that

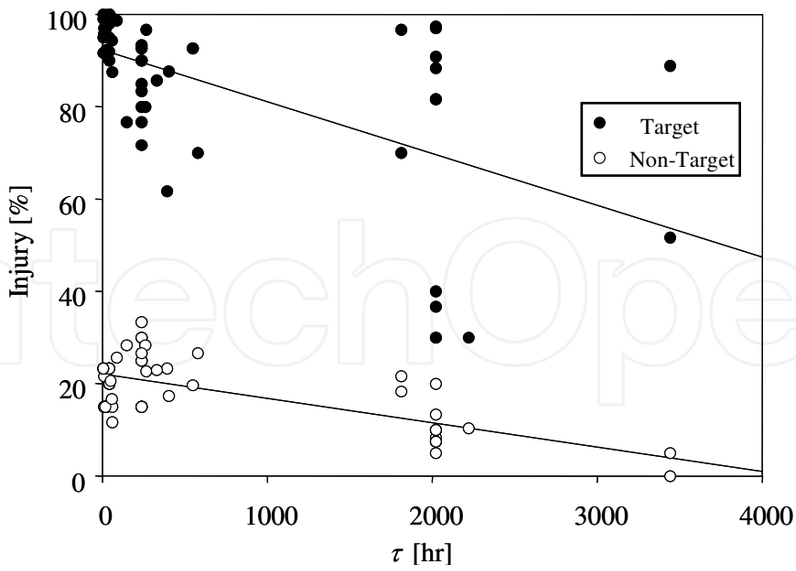

Fig. 6. Summary of greenhouse biological and laboratory determined release rate (τ= release half life) observations of plant injury for a commercial herbicide.

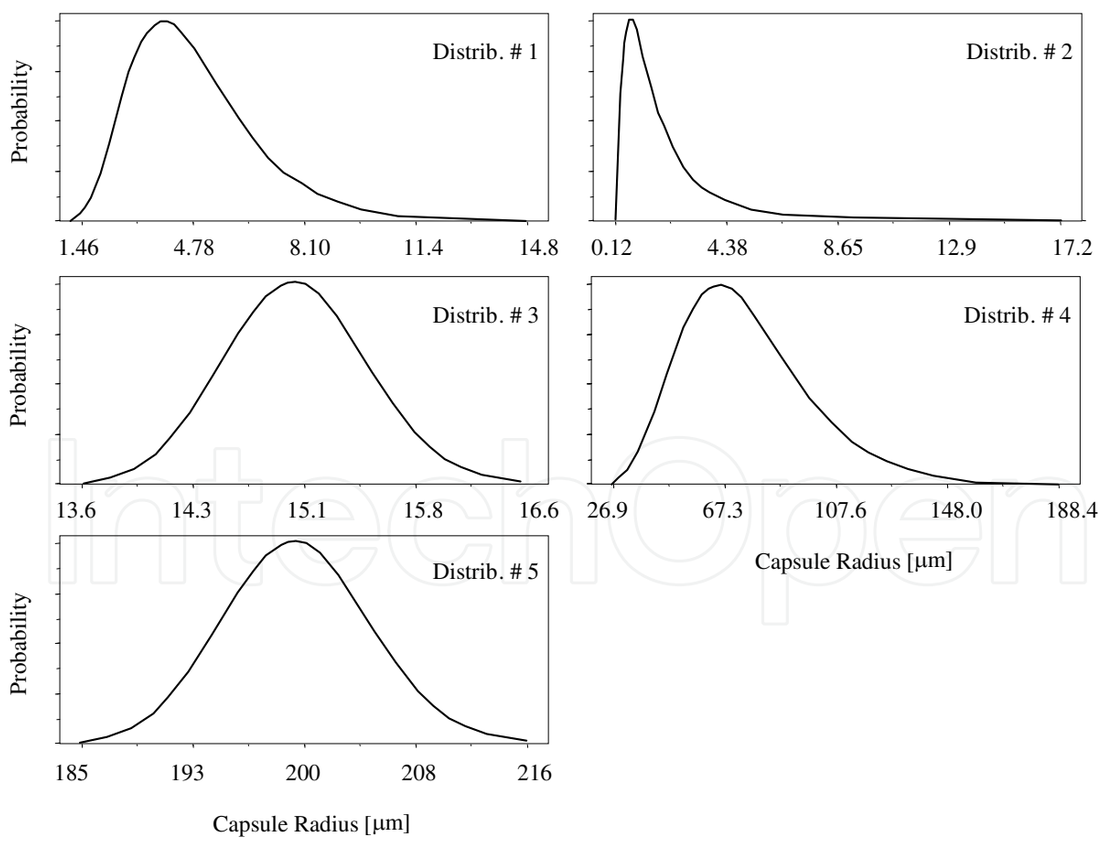

Fig. 7. Five capsule size distribution [radius (μm)] used in text example. The mean (μ) and standard deviation (σ) for all five distributions, given in increasing order are (5, 2), (2,2), (15, 0.5), 75, 25), (200, 5) for distributions 1-5, respectively.

approximated in greenhouse trials [e.g., τ_0 = 504 h = 21d]. The optimal concentration functions seen in Figure 8 represent predictions when γ and β are allowed to vary, and the application rate for field predictions is equal to that of greenhouse trials. The Solver routine of Microsoft excel (Branch and Bound solution technique) was employed to estimate the "optimal" parameter combinations for capsule mass fraction (f_i), γ, and β such that the objective function (Eq. 18) was minimized.

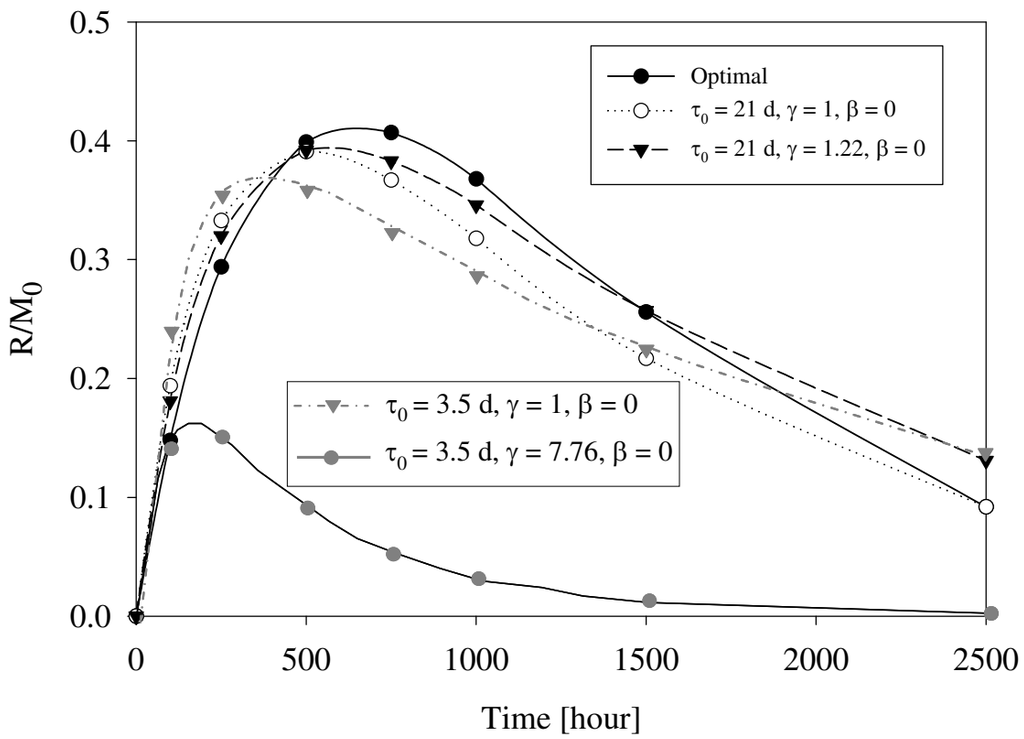

Fig. 8. Greenhouse determined optimal environmental matrix concentration with predicted "optimal" capsule formulation combinations when environmental degradation half-life (τ_0) is 21 or 3.5 days. γ and β parameters from Eq. 17.

Different mass fractions for capsule distributions of various sizes (e.g. Figure 7) ensue for each optimal calculation. Optimization results are summarized in Table 1 with optimal selection of mass fractions for the five different size formulations also provided. However, optimal results suggest the amount of conventional formulation added to the capsule formulations should be zero (β =0), and the resulting predicted concentration profile is similar to the biological optimal. Thus, one would expect field behavior for the first two entries found in Table 1 to yield similar results to greenhouse observations for this choice of inputs (assuming field dissipation occurs at a half-life of 21 days).

For the commercial herbicide used, the field dissipation half-life is approximately 3.5 days, while the green house aerobic aquatic half-life was estimated at 21 days. Therefore, one should *a priori* expect dramatically different behavior will ensue under field conditions. To appropriately mimic field behavior, the dissipation half-life was set to 3.5 days and the procedure for selecting mass-fractions of capsule distributions was repeated. Results of this exercise are also represented in Figure 8 and Table 1. What is evident in Figure 8 is the

disparity between results for the optimal release (where degradation had a 21-day half-life) versus the simulated field trial where the degradation half-life is 3.5 days. If the same amount of mass is used as in the biological trials (α=1, β =0), then the optimal release pattern using combinations of 5 different capsule distributions is poor. One would thus anticipate failure in field trials under these conditions before a field study is even initiated.

τ_0 [days]	β	γ	Optimal Mass Fraction (f_i)	ψ
21	0	1	(0.898, 0, 0.102, 0 , 0)	0.0093
21	0	1.22	(0.653, 0, 0.347, 0, 0)	0.0042
3.5	0.119	1	(1, 0, 0, 0, 0)	0.41
3.5	0	1	(1, 0, 0, 0, 0)	0.41
3.5	0	7.76	(0, 0, 1, 0, 0)	0.030

Table 1. Optimal mass fractions for capsule distribution combinations of text problem, along with ratios of conventional formulation (β) and application rate increases above greenhouse observations (γ).

The degradation pattern under field conditions is so rapid that the maximum concentration in the environmental matrix never reaches that observed for the biological observation studies. However, this limitation can be overcome if more mass is added into the system. When γ and β are allowed to vary, the optimal combination of capsule distributions more closely matches results where biological information is available. In this example, when the optimal results of γ = 7.76 and β = 0 are used, one would expect similar biological effects as what was observed in the greenhouse trials. Thus, the amount of mass applied should be ~7.76 times that used in the biological greenhouse trials, with no conventional formulation added. If the greenhouse trial had an application rate of 10 g ha^{-1}, then the field trial using the combination of capsule distributions for this example should have an application rate of ~ 10×7.76 = 77.6 g ha^{-1}.

5. Microcapsule clustering

The prior analysis assumed interactions between neighboring capsules was negligible. However, the release rate of pesticide from microcapsules into the environment slows as the concentration driving force for mass transfer decreases (e.g. density of neighboring capsules increases). Therefore, quantifying the geometries of microcapsule clusters and the resulting pesticide release rate from such clusters is paramount for realistic estimates of pesticide release.

Clustering of solid particles can occur in two phase systems (liquid, solids) where one phase (liquid) is responsible for transport of the second phase (solids). Microcapsules are mixed with water and delivered to the target site via conventional spray application equipment, where the spray drops now contain microcapsules. Following delivery, sessile drops (drops resting on a solid surface) containing microcapsules evaporate. During the evaporation process, microcapsules within the drop are transported to the drop contact line by capillary-induced convective flow patterns, thus forming annular rings of microcapsule clusters upon drop evaporation. The phenomena of the "coffee ring", where macroscopic patterns of fine particles arise as a drop containing the particles evaporates, was first explained by Deegan

et al (1997). Numerical solutions to this problem have been documented (Hu and Larson, 2002; Widjaja and Harris, 2008). Solid particle clustering was further quantified by alternative mechanisms dictated by hydrodynamics of the liquid phase (Kondic and Murisic, 2008). Capillary-induced convection provides a mechanism to organize suspended particles that range from nanometers to micrometers (Maillard et al, 2001; Small et al, 2006) and has been used to optimize ink jet printing and to create self-assembling micro and nano-structures (Dufresne et al, 2003; Tsukruk et al, 2004), and in understanding the crystalline patterns that form following drying droplets of DNA which are stretched and subsequently deposited for gene expression profiling (Smalyukh et al, 2006). Additionally, the impact of Marangoni (surface tension) gradients at the drop interface has been shown to reverse the formation of the "coffee-ring" deposits (Hu and Larson, 2006).

Flow patterns set up within an evaporating sessile drop, responsible for microcapsule movement and clustering, have been proposed. A unidirectional, one-dimensional radial flow from the sessile drop center to the drop edge was suggested as being responsible for the clustering of solid particles near the pinned, wetted perimeter. This analysis assumes lubrication theory and with evaporation described by a Laplace equation (Deegan et al., 1997; Deegan et al. 2000; Popov, 2003; Popov, 2005). A two-dimensional analytical expression for the hydrodynamic potential inside an evaporating spherical sessile drop with a pinned contact line, represented as a Fourier-Legendre series expansion, has also been proposed (Tarasevich, 2005). A necessary input parameterizing this velocity potential is the rate of change in the spherical cap with respect to time. Both drop dimensions and the rate of change of the sessile drop height over time are easily measured or calculated using experimental values (Cryer and Wilson, 2009).

6. Experimental

6.1 Microcapsule construction

Microcapsules were prepared by standard interfacial/condensation polymerization where the membrane wall was formed by the reaction of polymeric diphenylmethane-4, 4'-diisocyanate (polymeric MDI (polymethylene polyphenylisocyanate); PAPI 27 (Dow Chemical); oil soluble monomer) with diethylene triamine (DETA; water soluble monomer) to form a polyurea. The oil used was Aromatic 100 without any dissolved pesticide to produce "blank" microcapsules. Differing amounts of mixing shear were performed to create an emulsion (water, surfactant, solvent (oil) and oil soluble monomer) having different size distributions. Subsequent polymerization occurs when the water soluble monomer was added. A Malvern Instruments Mastersizer 2000 particle size analyzer recorded the capsule size distributions for the formulations used in this analysis. Two different size distributions, having mean diameters of 2 or 10-μm, respectively, were created to approximate size distributions associated with commercial agricultural formulation microcapsules, with both displaying multi-modal behavior (Figure 9).

6.2 Visualization system for microcapsule clustering

Water drops (0.5μl – 5 μl) containing microcapsules were placed on glass slides using a 10 μl syringe. Drop evaporation and microcapsule clustering following evaporation were analyzed using an Olympus Privis AX70 Microscope with 10x, 20x, 40x, 60x, and 100x optics and a Sony 3CCD color video camera (Model DXC-970MD). A TA instruments TGA 2050 (Thermal Gravimetric Analyzer) was used to measure water drop evaporation rates.

Multiple replications for room temperature evaporative mass losses for several sizes of distilled water droplets (1 μl, 5 μl) were measured. Drop volumes were representative of volumes of agricultural spray nozzle output.

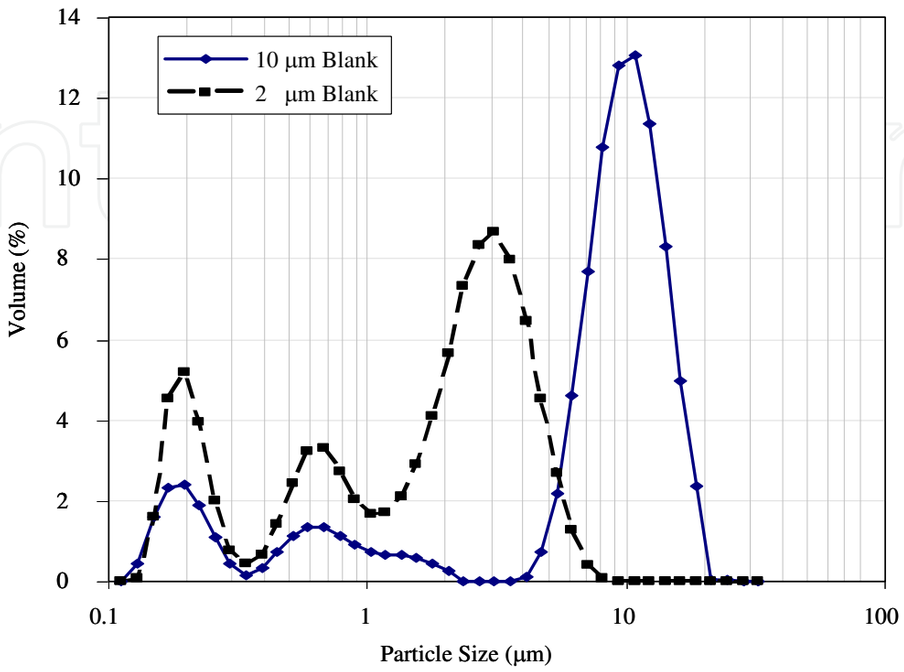

Fig. 9. Capsule particle size distribution for mixtures labeled as either 2- or 10- μm (mean) diameter.

By visual observation, the contact line for a water droplet containing microcapsules was pinned during the entire evaporation process, and there were always a higher percentage of smaller diameter capsules observed near the perimeter edge post evaporation, Figure 10. Microcapsules were generally segregated by size as one travels from the wetted perimeter edge toward the center of the wetted area. Of interest was the fact that indeed a "coffee stain" shape of a single layer thickness of microcapsules forms following evaporation of the water carrier. Only single layers of capsules (e.g., a monolayer of 2-dimensions) were observed for all experimental observations. Neutrally buoyant capsules of different sizes travel at the same velocity within the water drop flow field, with smaller capsules penetrating closer to the drop perimeter edge before eventually succumbing to the interfacial force strength once a portion of the capsule extends beyond the water/air interface. Larger capsules succumb to the interfacial force before smaller capsules as both approach the pinned contact line due to the curvature and depth of the carrier drop along the edge (Cryer and Wilson, 2009).

Experimental observations of microcapsule placement following drop (water) evaporation illustrate microcapsules cluster in monolayers at the former (original) pinned contact line of the drop. The radius of the pinned contact line is a function of both the solvent/solid contact angle and the drop size/volume. Surface tension impacts the starting shape of the sessile drop, and thus can impact capsule movement and possible clustering during evaporation.

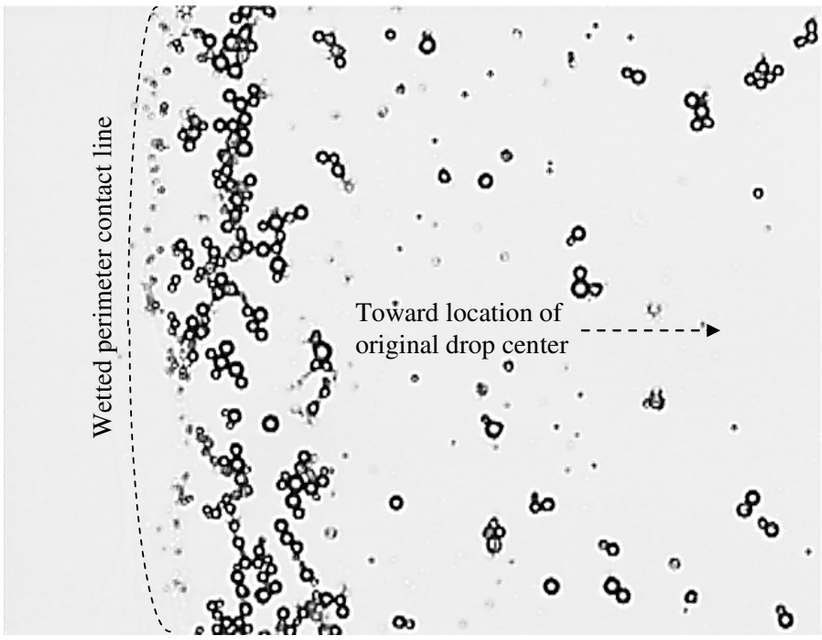

Fig. 10. Example of 10 μm (average diameter) capsule clusters near a portion of the wetted perimeter edge following evaporation of a 1 μL sessile drop (looking down onto the solid surface).

7. Theoretical

The sessile drop is approximated as a spherical cap having a pinned contact line. As the drop evaporates, the resulting spherical cap is modeled as a series of constrained quasi-static equilibrium shapes. Mass loss for pure water droplets (evaporation) was linear over time (Cryer and Wilson, 2009). This linear rate of mass loss yields the transient rate of volume change (dV/dt) and height (dh/dt) of the evaporating drop which was used to determine velocities within the drop. The evaporation rate of water was sufficiently small that a quasi-static approximation for the dynamic behavior for changes in drop shape during evaporation is valid. The change in the spherical cap height with respect to time for a sessile drop having a pinned contact line is linear under quasi-static assumptions, e.g.

$$\frac{d\,h}{d\,(t\,/\,t_f)} \cong h_0\,. \tag{19}$$

where h_0 is the rate of change of the spherical cap height with respect to time (t), and t_f is the time when the sessile drop fully evaporates. Only for contact angles ≥ 90° do small deviations from linearity arise. Thus, the rate of mass loss is proportional to the height of the spherical cap (Rowan et al, 1995), and not the spherical radius for the sessile drop.

7.1 Microcapsules transport via convective patterns from sessile drop evaporation

Capillary-driven velocity profiles within an evaporating sessile drop require characterization if quantitative predictions for microcapsule clustering and subsequent pesticide release rate are sought. The sessile drop was considered a spherical cap since the

gravitational effect on small droplets on the order of 5-μL was negligible (Bond Number <<1). The spherical cap geometry is dictated by the contact angle of the drop with the soil surface, Figure 11 (a), where the volume is held fixed but the contact angle is allowed to vary. As θ decreases, the drop spreads more readily on the solid. If the wetted perimeter contact line remains fixed as the water evaporates, equilibrium shapes for the drop can be calculated, Figure 11 (b). In the nomenclature for a spherical cap, Figure 11 (c), x is the radius of the contact perimeter, h is the height of the spherical cap, θ is the contact angle of the water drop with the solid surface, and R is the radius of the sphere used to describe the drop. The value of x remains constant for a pinned contact line, and only the values of θ, h and R change as the carrier drops evaporate. Geometric constraints dictate

$$h = R\,(1\text{-}\cos\theta) \tag{20}$$

$$x \equiv R \sin\theta = R_0 \sin\theta_0 \tag{21}$$

and that time is scaled by volume changes. Thus

$$\frac{t}{t_f} = 1\text{-}\frac{V}{V_0} \tag{22}$$

where t_f = time when all of the liquid within the drop has evaporated, and the volume of spherical cap (V) is

$$V = \frac{1}{3}\pi h^2(3R\text{-}h) = \frac{\pi}{3} R^3(1\text{-}\cos\theta)^2(2+\cos\theta). \tag{23}$$

The initial parameters for the drop volume, spherical cap radius and height, and the contact angle (V_0, R_0, h_0, θ_0), denote the drop shape at the onset of evaporation (e.g., stationary drop immediately following placement on a solid substrate such as a leaf surface) and were assumed known via analytical solutions to the spherical cap approximation or the Laplace-Young equation for a given volume (V_0) and contact angle constraint (θ_0).
V_0 = volume of the drop at time = 0.
R_0 = Radius of sphere describing drop (spherical cap) at time = 0.
h_0 = height of spherical cap at time = 0.
θ_0 = contact angle of drop at time = 0.
Velocity magnitudes responsible for microcapsule movement were approximated by the Laplace flow generated within the drop (pinned contact line) as it evaporates using the analytical flow potential of Tarasevich (2005), Figure 12. Microcapsule trajectories within this flow field were coupled with the vertical buoyancy/gravity components for the microcapsule to yield the microcapsule trajectory within the evaporating sessile drop. A neutrally buoyant capsule will follow the flow streamlines, while a capsule whose bulk density is greater or less than that of the carrier will generate patterns that deviate from the flow streamlines. It was assumed microcapsules do not significantly alter the underlying base flow that was derived for a single phase fluid. Details for the capsule force balance within the imposed velocity field is summarized elsewhere (Cryer and Wilson, 2009).

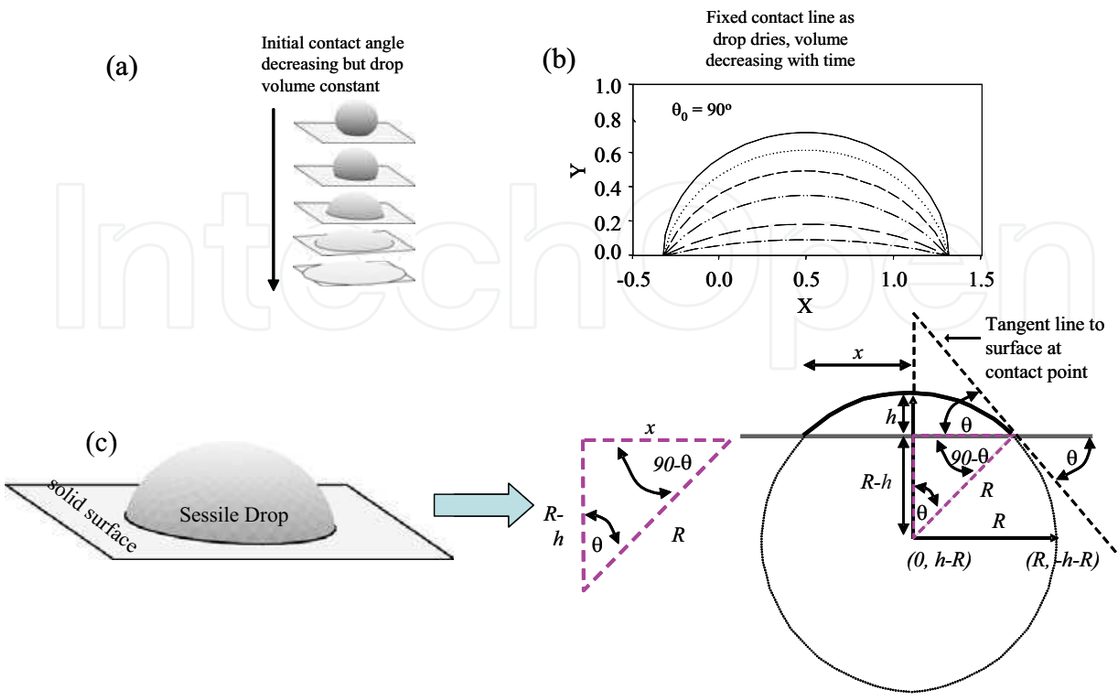

Fig. 11. Nomenclature for sessile drop approximation as a spherical cap.

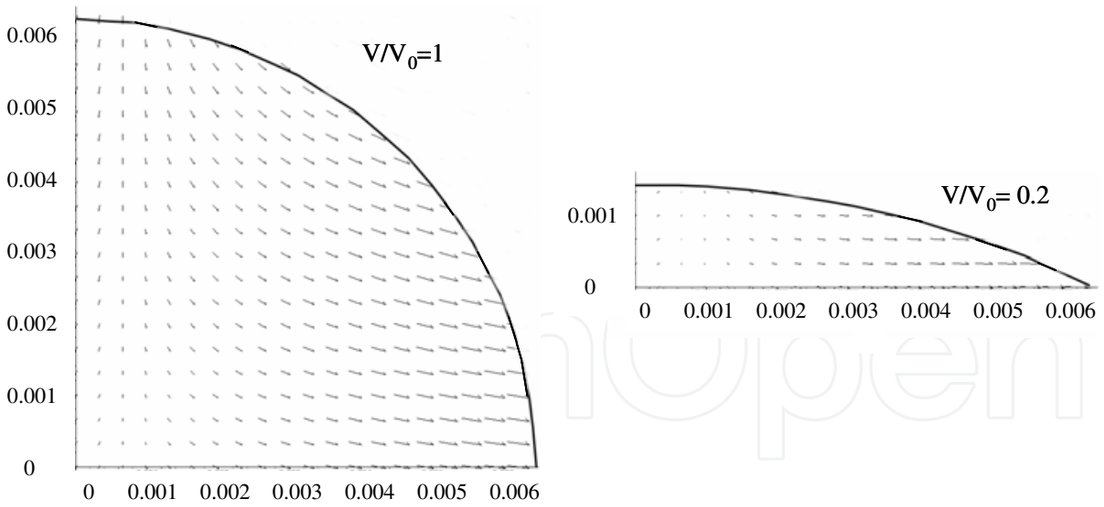

Fig. 12. Example of equilibrium shape sessile drops for fixed volume but different contact angles and for a pinned contact line (a) for evaporating drop. Analytical solution for velocity profile for drying drop simulated as a quasi-static spherical cap. Initial contact angle of 90° ($V/V_0 = 1$) with a drop volume of 2-µl.

For simulation purposes, an equilibrium-shaped sessile drop at the onset of evaporation had 1000 microcapsules uniformly distributed within the drop. Each microcapsule location and the transient interface shape was tracked over time steps as the drop evaporated. Estimates

of the width of the annular ring of microcapsule clustering were obtained by following the travel distance of a unique microcapsule until the water fully evaporated and convective forces responsible for transport ceased. Thus, the percentage of starting microcapsules that are transported to the wetted perimeter following evaporation is known. The numerical system was executed for different drop sizes and initial contact angles.

Larger volume drops typically have 100% of the initial uniformly distributed microcapsules transported to the pinned, wetted perimeter edge. The percentage of microcapsules reaching the wetted perimeter edge before the drop fully evaporates decreases as the water drops decrease in volume, Figure 13. There is a competition between microcapsule transport and drop evaporation. Larger drops take longer to fully evaporate and thus offer more time for capsules to reach the pinned contact line. The quasi-static mathematical description used to approximate the velocity fields within an evaporating sessile drop suggests microcapsule transport and the formation of the annular ring of microcapsules was a function of initial drop size, capsule number density, and the equilibrium contact angle, and perhaps the locations of microcapsules within the sessile drop as the drop initially comes to rest.

The droplet size distributions for conventional agricultural nozzles (shaded area, Fig. 13) represent the very fine to coarse droplet size distribution classes obtained from atomization

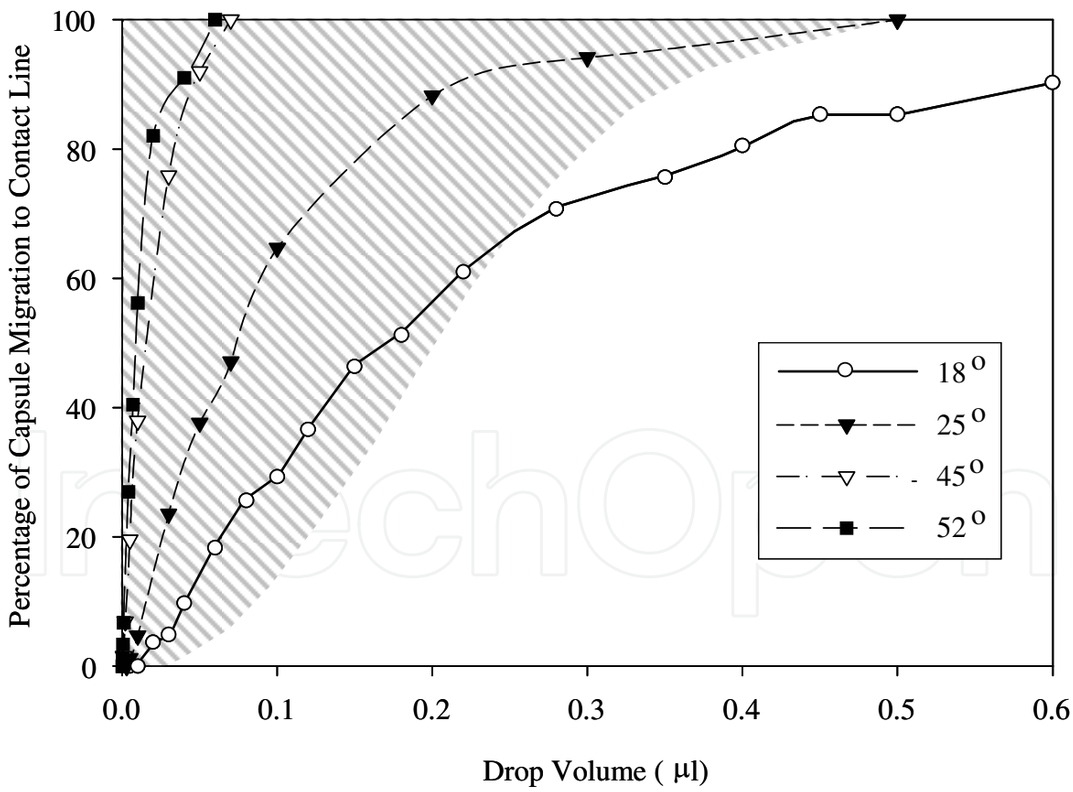

Fig. 13. Percentage of uniformly dispersed microcapsules predicted to migrate to pinned contact line following solvent evaporation as a function of initial contact angle. Shaded area represents agricultural nozzle droplet sizes classified from very fine to coarse.

experiments (Doble et al., 1985). Thus, all spray nozzles of agricultural importance yield drop diameters of sufficient size where a portion of the microcapsules within these carrier drops will cluster near the perimeter edge (observed experimentally and predicted numerically). Capsule clustering and the impact on pesticide release rate should not be ignored.

Often, a formulation that works under greenhouse and lab conditions fails when taken to the field. Microcapsule transport mechanisms in the evaporating sessile drop may provide a mechanism to address failure rates partially attributed to reduced pesticide release (and thus efficacy) resulting from capsule clustering. Microcapsules are more likely to be deposited in a uniform pattern across the entire wetted drop only as the water drop size decreases. Conventional microcapsule attributes and the self-assembly of microcapsule clustering in evaporating sessile drops can now be used to predict environmental concentrations of pesticides following release.

8. Coupling capsule clustering with pesticide release rate

Computational fluid dynamics (CFD) software (Fluent 6.3.26, ANSYS 2006) was used with the mass conservation equation (diffusion) to simulate pesticide mass transfer losses for seven specific clustered microcapsule geometries (Figure 14). Only the immediately adjacent capsules were considered in the analysis, thus providing a bound for higher release rate predictions. The darker shaded capsule in Figure 14 is the capsule of interest. Each capsule was assumed to have similar properties (i.e., radius, mass loading, membrane thickness, etc.), and the transient pesticide mass remaining within the capsule of interest was calculated over time. As the number of surrounding capsules increased, the overall pesticide release rate decreased.

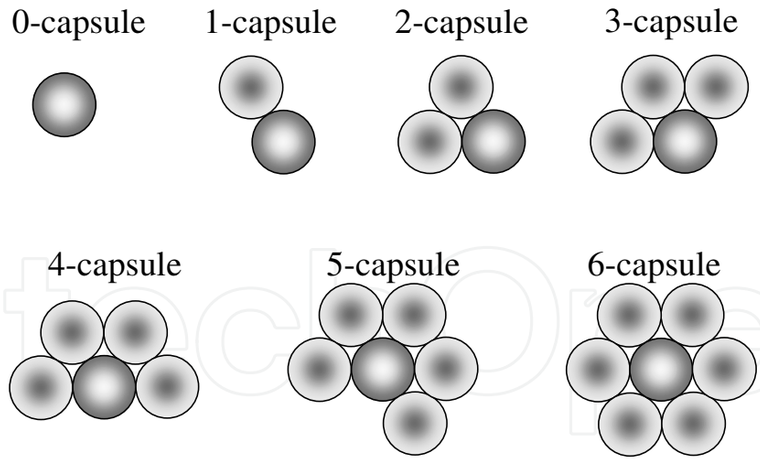

Fig. 14. Single microcapsule surrounded by 0-6 additional capsules.

The CFD model predicted release rates of decomposed 0-6 surrounding capsule clusters follow an exponential decay pattern with time and are summarized in Table 2. A simple exponential function (Eq. 24, $r^2 = 0.97$) was found to adequately represents the correlation between the number of capsules within a cluster and the scaled mass loss rate constant for a specific capsule (k_i/k_0).

$$k_i/k_0 = \exp[-0.187 * S_i)]. \quad (24)$$

S_i equals the integer number of surrounding capsules (integer value between 0-6, inclusive) since a single capsule rate constant (k_0) was theoretically known and is a function of polymer properties and membrane thickness (Eq. 7 when characteristic half-life is converted to a rate constant). Thus, different polymers and membrane thicknesses can be assumed, k_0 updated, and Eq. 24 used to estimate release losses as the number of surrounding capsules increases.

Number of surrounding capsules	a	k_i [d^{-1}]	r^2
0	0.8567	0.1467	0.8385
1	0.8532	0.1168	0.7951
2	0.8543	9.30E-02	0.7663
3	0.865	7.83E-02	0.7772
4	0.8753	6.90E-02	0.79706
5	0.8847	6.24E-02	0.82506
6	0.898	5.58E-02	0.8574

Table 2. Fit of CFD results to 1st order exponential decay model ($M/M_0 = a\, e^{-k_i t}$, where t is in days).

Specific cluster geometries were developed using an empirical random placement approach once experimental or numerical observations for representative capsules within a cluster were known. The number of individual microcapsules in a cluster (N_T) was defined by a probability density function (PDF) based upon experimental observations. The cluster was randomly grown, as illustrated in Figure 15, with N_T selected by Monte Carlo (MC) sampling of the PDF. The starting capsule of a cluster was placed at the origin (0, 0). There are four possible locations for the next capsule [(-1, 0), (0, 1), (1, 0), (0, -1)]. Each possibility has the same probability of being randomly selected for the next capsule location (although the probability for future capsule placement can likewise be weighted). For this example, the nodal point (1, 0) was chosen for the next capsule placement [Figure 15 (b)]. Now, there are six distinct locations where the next capsule can be randomly placed as illustrated by the gray nodes in Figure 15 (b). The procedure was numerically repeated until N_T capsules were contained in the cluster. Each capsule within the two-dimensional cluster has a characteristic number of surrounding capsules. Release for any monolayer capsule cluster was approximated based upon the decomposed cluster structures (e.g. Figure 14) and a weighted linear superposition for all (0-6) sub-capsule geometries represented.

A 17-cluster example is provided in Figure 16, illustrating the locations for the 3 unique capsules surrounded by 6 neighboring capsules contained within this unique cluster. Each capsule within the cluster was evaluated for neighbors, and the capsule net rate constant for pesticide release (k_{net}) was assumed to be a linear weighting of release rate constants for the smaller decomposed capsule geometries (e.g., Fig. 14).

$$k_{net} = \frac{1}{N_T} \sum_{i=1}^{6} N_i k_i \tag{25}$$

Here, N_i is the total number of unique decomposed capsule geometries having "i" surrounding capsules in the cluster, and k_i represents the release rate constant for the

decomposed capsule cluster geometry "i" estimated by CFD. An entire 2-dimensional cluster can be disseminated into unique numbers of individual 0-, 1-, 2-, 3-, 4-, 5-, and 6-capsule interaction-component building blocks whose CFD-predicted release profiles are known. The overall mass loss from the clusters varies depending upon physical properties of the capsule and pesticide (e.g. Equations 1-3), and cluster orientation and geometry since different cluster orientations (for a fixed N_T) can have different fractions (0-6) of capsule interaction.

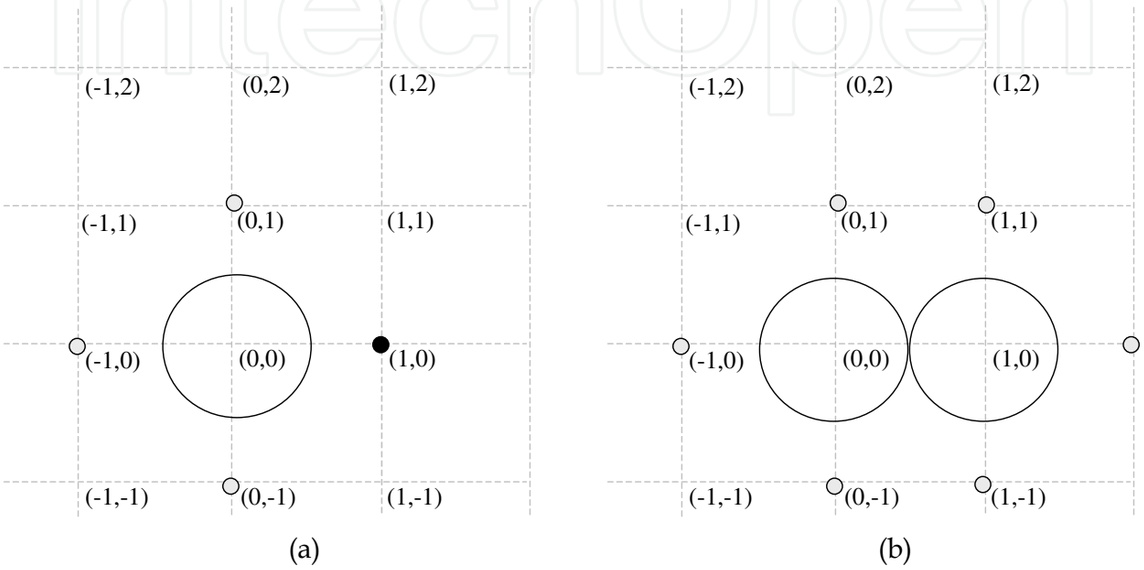

Fig. 15. Two-dimensional cluster formation based upon random placement of capsules with spatial coordinates scaled by the microcapsule diameter.

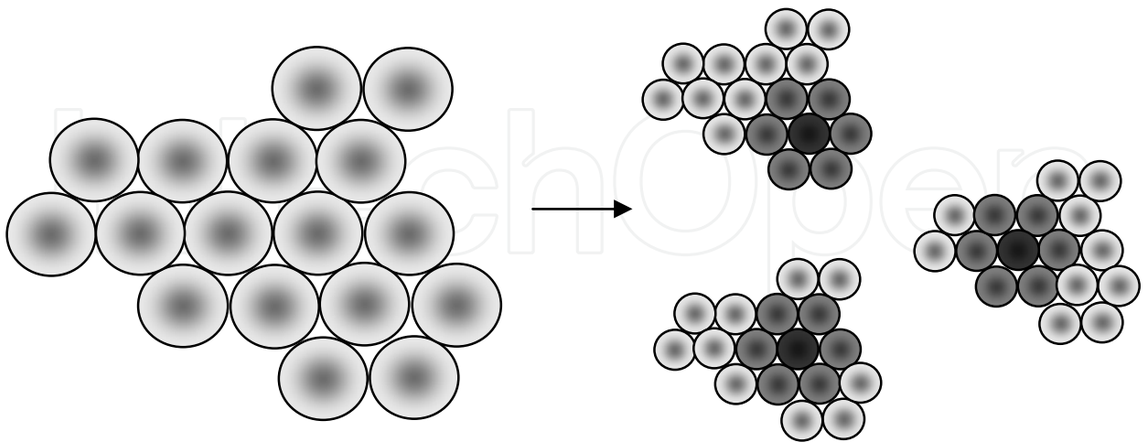

Fig. 16. Seventeen-capsule cluster illustrating how a single capsule can be isolated and the number of neighboring capsules deduced (a). Decomposition example for 17-capsule cluster into number of capsules surrounded by six neighbors.

Figure 17 illustrates results for a 17-capsule cluster using the proposed decomposition approach for the mass fraction of pesticide remaining within the capsule over time. The concentration gradient driving force for the central capsule of interest decreases as the number of surrounding capsules increases, and thus the mass loss for the central capsule decreases. Different cluster geometries have different release characteristics, even though the total number of capsules (N_T) for each cluster remains constant. In summary, the release rate and subsequent environmental concentration is a function of the capsule properties such as the initial loading, size, membrane thickness, diffusivities, environmental degradation of the pesticide once released, and the clustering of the micro-capsules as governed by convective patterns established during droplet evaporation following delivery to the target site.

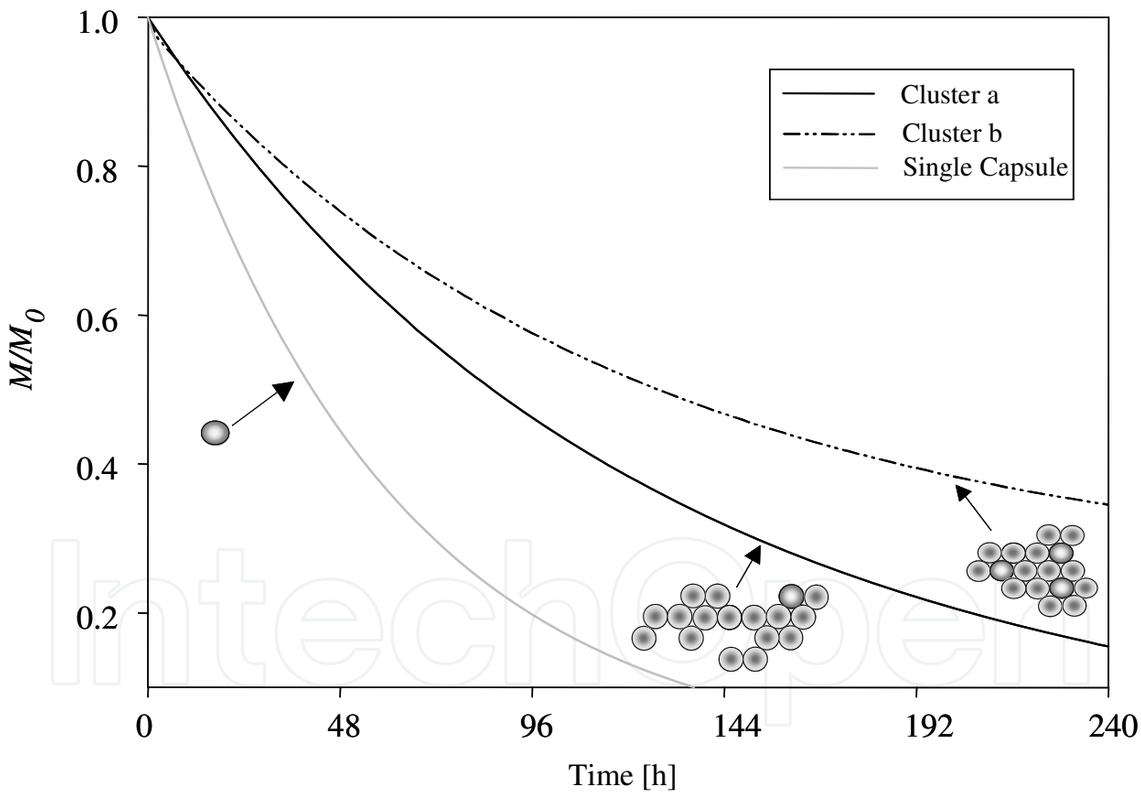

Fig. 17. Representative release loss from three different 17-capsule clusters. Physical properties for capsules are identical [only difference is in cluster structure, k_0 = 0.405 d^{-1} (k_0 is the release coefficient for a single capsule in an infinite medium)].

9. Discussion

Characterization of diffusion mass loss from a single microcapsule is straight forward and easily adaptable to distributions of different microcapsule sizes assuming capsule to capsule interactions are negligible. Conventional parameters that impact pesticide release include microcapsule size and polymer membrane properties. The modeling approach outlined in this chapter describing capsule clustering (e.g. the "coffee stain" following conventional application procedures) provides a mechanism to deduce capsule clustering and the impact clusters have on the overall pesticide release rate. Thus, optimal release patterns can be constructed to yield the desired biological effect that combines both formulation characteristics (e.g. capsule size, membrane thickness, pesticide loading) and application parameters (e.g. sessile drop size, contact angle with solid surface) since they are not mutually exclusive.

The coffee stain effect for microcapsules was altered by both capsule density and the drop size for the water carrier. Annular rings of microcapsules were observed as the carrier drop size decreased and/or the number density of capsules within the drop increased. Numerical or analytical approaches using the diffusion equation to predict pesticide release rates from single capsules would over predict losses from clustered microcapsules.

10. Conclusions

Physically-based diffusion models were developed to determine release loss from dilute systems of microcapsules of non-uniform radii. The diffusion coefficient across the capsule membrane can be indirectly approximated by these approaches if laboratory release data is gathered. The formulation release pattern is coupled with environmental fate information to calculate the transient concentration profile of the pesticide in the environment that can be subsequently compared to experimental profiles found to yield the biological effect of interest.

Formulation design was illustrated using a combination of five different microcapsule size distributions for a commercial herbicide where the optimal release profile was deduced based upon direct measurement of release characteristics and subsequent biological observations. This release profile and dissipation pattern under greenhouse conditions provided the basis for calculating an optimal environmental concentration profile under field conditions that would yield similar biological behavior. The methodology/model outlined in this chapter provides a mechanism for increasing the probability for successful extrapolation of greenhouse trials to field predictions through combinations of various capsule distribution sizes, conventional formulation additions, variable application rates, and accounting for environmental degradation/dissipation patterns. Multiple capsule distributions can be combined in an effort to mimic various concentration profiles in environmental matrices of interest. Conventional formulations (i.e., instantaneous release) and linear combinations of different size capsule distributions can be varied to obtain different environmental concentration patterns.

The effect of capsule clustering on release rate is an important mechanism that should be included for realistic predictions of pesticide release rates under field conditions. A first attempt at accounting for microcapsule clustering in two dimensions was presented. The

quasi-static approach used to model the dynamic behavior of the sessile drop shape during evaporation proved adequate to address observed clustering of microcapsules. A semi-empirical diffusion model was developed for estimating pesticide release loss from 2-dimensional clusters of microcapsules based upon numerical solutions to the diffusion equation. Predicted environmental release patterns are combinations of various capsule size distributions and geometries, polymer membrane thickness, pesticide loading, and environmental dissipation parameters. This coupling of microcapsule formulation attributes, formulation design, and capsule placement, with biological observations, can increase the likelihood for formulation success under field conditions. "Properly accounting for physical phenomena such as microcapsule clustering and its impact on pesticide release rate reduces efficacy uncertainty and the likelihood for undesirable behavior under a variety of different conditions."

11. References

Akelah, A. 1996. Novel utilizations of conventional agrochemicals by controlled release formulations. Materials Science and Engineering C. 4:83-98.

Allan, G.G. C.S Chopra, A.N. Neogi, R.M. Wilkins. 1971. Design and Synthesis of Controlled Release Pesticide-Polymer Combinations. *Nature*, Vol. 234, pp 349-351.

ANSYS, Inc. 2006. Fluent Computational fluid dynamics software. Santa Clara, CA.

Asrar, J.Y. Ding, R.E. La Monica, L.C. Ness. 2004. Controlled Release of Tebuconozole from a Polymer Matrix Microparticle: Release Kinetics and Length of Efficacy. J. Agric. Food Chem., 52(15):4814:4820.

Carslow, H.S.; J.C. Jaeger, 1959. Conduction of Heat in Solids. Clarendon Press, Oxford, England.

Collins, R.L; S. Doglia, 1973. Concentration of Pesticides Slowly Released by Diffusion. *Weed Science*. Vol 21, 4, pp. 343-349.

Collins, R.L. 1974. A Theoretical Foundation for Controlled Release. Controlled Release Pesticide Symposium. Engineering and Science Division, Community and Technical College, The University of Akron, Sept. 16-18, 1974.

Cowsar, D. R., 1981. Controlled Release: Benefits vs. Risks. Controlled Release of Pesticides and Pharmaceuticals. D.H. Lewis (Ed.). Plenum Press, New York and London.

Crank, J. 1993. The Mathematics of Diffusion, 2nd edition. Clarendon Press, Oxford.

Cryer, S.A. and S.L. Wilson. 2009. Modeling Approach to Assess Clustering Impact on Release Rates of Pesticides from Microencapsulated Products. J. Agricul. Food Chem. 57, 5443-5451.

Dailey, O.D., C.C. Dowler, B.G. Mullinix. 1993. Polymeric microcapsules of the herbicides atrazine and metribuzin: Preparation and evaluation of controlled-release properties. J. Agric. Food Chem.. 41 (9):1517-1522.

Dailey, O.D. 2004. Volatilization of Alachlor from Polymeric Formulations. J. Agric. Food Chem., 52(22):6742-6746.

Deegan, R.D.; O. Bakajin, T.F. ; Dupont, G. ; Huber, S. R. ; Nagel, T. A. Witten. 1997. Capillary Flow as the cause of ring stains from dried liquid drops. Nature 389, 827.

Deegan, R.D. ; O. Bakajin, T.F. Dupont ; G. Huber, S.R. Nagel; T.A. Witten. 2000. Contact line deposits in an evaporating drop. Physical Review E, 62, 1, pp. 756-765.

Doble, S.J. ; G.A Mathews, I. Rutherford, E.S.E Southcombe. 1985. A system for classifying hydraulic nozzles and other atomizers into categories of spray quality. Proceedings of the British Crop Protection Conference, Weeds, 3:1125-1133.

Dowler, C.C., O.D. Dailey, B.G. Mullinix. 1999. Polymeric Microcapsules of Alachlor and Metolachlor: Preparation and Evaluation of Controlled-Release Properties. J. Agric. Food Chem., 47(7):2908-2913.

Dufresne, E. R.; E.I. Corwin,. N.A. Greenblatt.; J. Ashmore, D.Y. Young,.A.D. Dinsmore, J.X. Cheng, X.S. Xie, J.W. Hutchinson,.D.A. Weitz. 2003. Flow and Fracture in Drying Nanoparticle Suspensions. Phys. Rev. Lett. 91, 224501

Hu H.; R.G. Larson. 2002. Evaporation of a sessile droplet on a substrate. J Phys Chem B. 106:1334-1344.

Hu. H. ; R.G. Larson.. 2006. Marangoni Effect Reverses Coffee-Ring Depositions. J. Phys. Chem. B, Vol. 110, No. 14, 7090-7094.

Kondic, L., N. Murisic. 2008. On Modeling Evaporation of Sessile Drops. AIChE annual meeting, Philadelphia, PA. Nov. 16-21, 2008.

Kydonieus, A.F. 1980. Fundamental Concepts of Controlled Release. Controlled Release Technologies: Methods, Theory, and Applications, Volumes I. pp. 1-19. Kydonieus, A.F. (Ed.) CRC Press, Inc. Boca Raton, Florida.

Maillard, M., L. Motte, M.P. Pileni. 2001. Rings and Hexagons Made of Nanocrystals, Adv. Mater 13, 3, pp. 200-204.

Mogul, M.G., H. Akin, N. Hasirci, D.J. Trantolo, J.D. Gresser, D.L. Wise. 1996. Controlled release of biologically active agents for purposes of agricultural crop management. Resources, Conservation and Recycling, 16:289:320

Muro-Sune, N. R. Gani, G. Bell, I. Shirley. 2005. Predictive property models for use in design of controlled release of pesticides. Fluid Phase Equilibria, 228-229:127-133.

Muro-Sune, N. R. Gani, G. Bell, I. Shirley. 2005. Model-based computer-aided design for controlled release of pesticides. Computers and Chemical Engineering 30, 28-41.

Popov, Y.O. 2003. Singularities, Universality, and Scaling in Evaporative Deposition Patterns Ph.D. Dissertation, Dept. of Physics, University of Chicago, Chicago, Illinois.

Popov, Y.O. 2005. Evaporative deposition patterns: Spatial dimensions of the deposit. Physical Review E, 71, 036313.

Quaglia, F., F. Barbato, G. De Rosa, E. Granata, A. Miro, M. Imacolata La Rotonda. 2001. Reduction of the Environmental Impact of Pesticides: Waxy Microspheres Encapsulating the Insecticide Carbaryl. J. Agric. Food Chem., 49(10):4808-4812.

Rowan, S.M., M.I. Newton, G. McHale. 1995. Evaporation of Microdroplets and the Wetting of Solid Surfaces. J. Phys. Chem. 99, 13268-13271.

Small, W.R., C.D Walton, J. Loos, M. in het Panhuis. 2006. Carbon Nanotube Network Formation from Evaporating Sessile Drops. J. Phys. Chem. B. 110, 13029-13036.

Smalyukh, I.I, O.V. Zribi, J.C. Butler, O.D. Lavrentovich,. G.C.L. Wong. 2006. Structure and Dynamics of Liquid Crystalline Pattern Formation in Drying Droplets of DNA. Physical Review Letters, 96, 177801.

Tsukruk, V.V., H. Ko, S. Peleshanko. 2004. Nanotube Surface Arrays: Weaving, Bending, and Assembling on Patterned Silicon. Phys. Rev. Lett. 92, 065502

Tarasevich, Y.Y. 2005. Simple analytical model of capillary flow in an evaporating sessile drop. Phys. Rev. E 71, 027301.

Widjaja, E., M.T. Harris. 2008. Particle Deposition Study During Sessile Drop Evaporation. AIChE J. 54:9, 2250-2260.

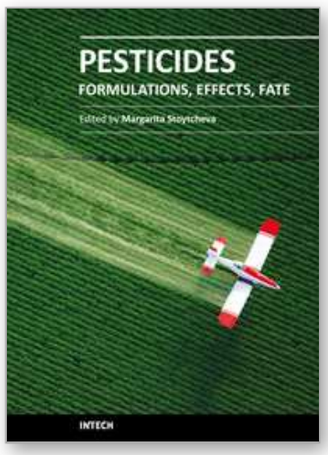

Pesticides - Formulations, Effects, Fate

Edited by Prof. Margarita Stoytcheva

ISBN 978-953-307-532-7
Hard cover, 808 pages
Publisher InTech
Published online 21, January, 2011
Published in print edition January, 2011

This book provides an overview on a large variety of pesticide-related topics, organized in three sections. The first part is dedicated to the "safer" pesticides derived from natural materials, the design and the optimization of pesticides formulations, and the techniques for pesticides application. The second part is intended to demonstrate the agricultural products, environmental and biota pesticides contamination and the impacts of the pesticides presence on the ecosystems. The third part presents current investigations of the naturally occurring pesticides degradation phenomena, the environmental effects of the break down products, and different approaches to pesticides residues treatment. Written by leading experts in their respective areas, the book is highly recommended to the professionals, interested in pesticides issues.

InTech Europe
University Campus STeP Ri
Slavka Krautzeka 83/A
51000 Rijeka, Croatia
Phone: +385 (51) 770 447
Fax: +385 (51) 686 166
www.intechopen.com

InTech China
Unit 405, Office Block, Hotel Equatorial Shanghai
No.65, Yan An Road (West), Shanghai, 200040, China
中国上海市延安西路65号上海国际贵都大饭店办公楼405单元
Phone: +86-21-62489820
Fax: +86-21-62489821

IntechOpen